On the Magnetic Ground State of La0.85Sr0.15CoO3 Single Crystals

ARTICLE *in* THE JOURNAL OF PHYSICAL CHEMISTRY C · JUNE 2011

Impact Factor: 4.77 · DOI: 10.1021/jp201206a

5 AUTHORS, INCLUDING:

Kaustuv Manna
Max Planck Institute for Chemical Physics of…
11 PUBLICATIONS **29** CITATIONS

SEE PROFILE

Anil PS Kumar
Indian Institute of Science
128 PUBLICATIONS **1,448** CITATIONS

SEE PROFILE

THE JOURNAL OF PHYSICAL CHEMISTRY C

ARTICLE

pubs.acs.org/JPCC

On the Magnetic Ground State of $La_{0.85}Sr_{0.15}CoO_3$ Single Crystals

Kaustuv Manna,[†] Debakanta Samal,[†] Suja Elizabeth,[†] H. L. Bhat,[†,‡] and P. S. Anil Kumar*[,†]

[†]Department of Physics, Indian Institute of Science, C V Raman Avenue, Bangalore 560012, India

[‡]Centre for Soft Matter Research, Prof. U. R. Rao Road, Jalahalli, Bangalore 560013, India

ABSTRACT: We present an extensive study on magnetic and transport properties of $La_{0.85}Sr_{0.15}CoO_3$ single crystals grown by a float zone method to address the issue of phase separation versus spin-glass (SG) behavior. The dc magnetization study reveals a kink in field-cooled magnetization, and the peak in the zero-field-cooling curve shifts to lower temperature at modest dc fields, indicating the SG magnetic phase. The ac susceptibility study exhibits a considerable frequency-dependent peak shift (~4 K) and a time-dependent memory effect below the freezing temperature. In addition, the characteristic time scale τ_0 estimated from the frequency-dependent ac susceptibility measurement is found to be $\sim 10^{-13}$ s, which matches well with typical values observed in canonical SG systems. The transport relaxation study evidently demonstrates the time-dependent glassy phenomena. In essence, all our experimental results corroborate the existence of SG behavior in $La_{0.85}Sr_{0.15}CoO_3$ single crystals.

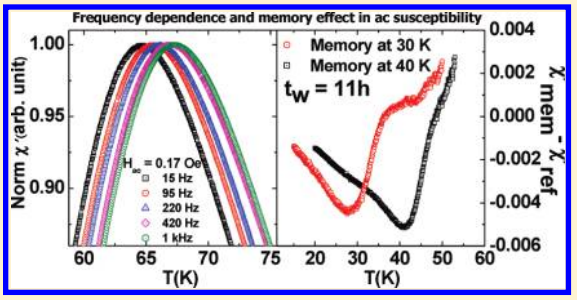

I. INTRODUCTION

The physics of doped transition-metal perovskites has been an area of intense research in the last few decades due to their interesting magnetic and transport properties.[1−3] Nevertheless, the magnetic ground state of some of these compounds continues to be a subject of debate even today. The most remarkable properties, such as colossal magnetoresistance (CMR) observed in manganites[1,3,4] and high T_c superconductivity[5] in cuprates, have revolutionized the understanding of the electronic correlation effects in such oxide systems. Though cobaltites do not exhibit the CMR effect like manganites, the temperature-dependent spin-state transition[6,7] and unusual magnetic ground state have made these systems more fascinating in terms of fundamental study. The temperature-induced spin-state transition from a low-spin state [LS: Co^{3+} ($t_{2g}^6e_g^0$; $S = 0$), Co^{4+} ($t_{2g}^5e_g^0$; $S = 1/2$)] to a more likely intermediate spin state [IS: Co^{3+} ($t_{2g}^5e_g^1$; $S = 1$), Co^{4+} ($t_{2g}^4e_g^1$; $S = 3/2$)] or a high spin state (HS: Co^{3+} ($t_{2g}^4e_g^2$; $S = 2$), Co^{4+} ($t_{2g}^3e_g^2$; $S = 5/2$)] arises due to the subtle competition between comparable sizes of the crystal field splitting (Δ_{CF}) and the intra-atomic Hund's exchange (Δ_{ex}) energy.[8−12] Again, one further layer of richness is added to the spin-state transition issue in rare earth cobaltites $R_{1-x}A_xCoO_3$ (R = lanthanide; A = alkaline earth, that is, Sr^{2+}, Ca^{2+}, or Ba^{2+}) depending on the size of the R ion.[13] It is found that, as the size of the R ion decreases, the lattice symmetry changes from rhombohedral to orthorhombic and the Co−O−Co bond angle deviates from 180°.[12,14] This can strongly affect the spin-state transition by changing the Δ_{CF} at the Co site. Among all the rare earth cobaltites ($R_{1-x}A_xCoO_3$), $La_{1-x}Sr_xCoO_3$ has attracted much attention due to its rich, but puzzling, phase diagram.[6,15] The parent compound $LaCoO_3$ is a charge-transfer type nonmagnetic insulator.[16] With the increase of Sr^{2+} doping concentration (x), the system evolves from the nonmagnetic state to the magnetic state. Most of the earlier studies show that, at $x < 0.18$, the system exhibits characteristics of semiconducting SG behavior and, at $x \geq 0.18$, it shows the metallic behavior with long-range ferromagnetic (FM) ordering.[15,17] In addition, in recent years, there is a strong conviction that the $La_{1-x}Sr_xCoO_3$ system exhibits magnetic phase separation (PS), that is, the partial coexistence of ferromagnetic metallic regions and nonferromagnetic insulating regions. This led to a renewed interest in examining the origin of the PS scenario in this system from both experimental and theoretical points of view. Different experimental techniques, such as NMR,[13,18] neutron diffraction,[19] magnetic relaxation,[20,21] and dc magnetization studies,[22,23] have established the existence of PS in these compounds. A few theoretical studies also support the existence of electronic and magnetic PS even in the absence of chemical PS.[24] Though there is incessant investigation in this direction, the complete knowledge about the detailed phase diagram of this system is still under debate.[6,15,17] Magnetically, the $x = 0.15$ composition lies in the border of SG and FM regions in the phase diagram of $La_{1-x}Sr_xCoO_3$. In the past few years, there is persistent debate among different research groups on its real ground-state magnetic property. Whereas some show evidence of PS, others report spin-glass behavior. Different research groups, such as Wu et al.,[22] Mira et al.,[27] and Caciuffo et al.,[14] endeavored to establish the presence of intrinsic PS in polycrystalline as well as single-crystalline[25,26] materials. They concluded that the origin of magnetic anomalies in this system is by virtue of redistribution of charges and phase separation into nanoscopic ferromagnetic clusters embedded in a nonferromagnetic matrix. Anil Kumar et al.[28] attributed compositional

Received: February 6, 2011
Revised: May 25, 2011
Published: June 13, 2011

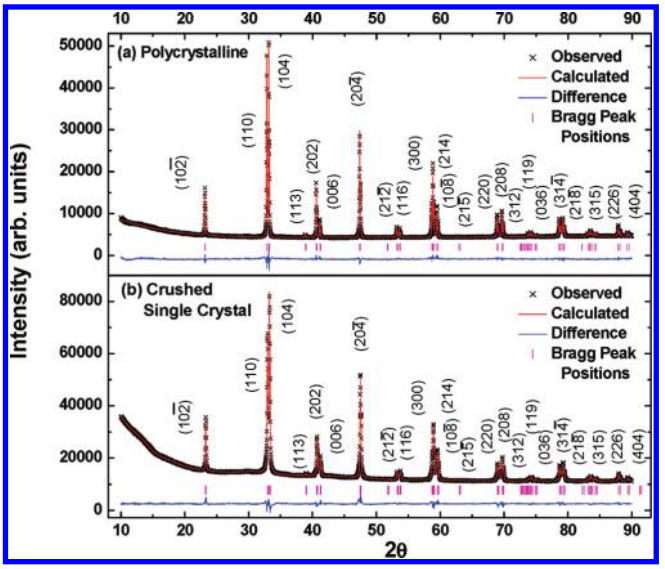

Figure 1. Rietveld refined profiles for powder X-ray diffraction patterns of $La_{0.85}Sr_{0.15}CoO_3$: (a) polycrystalline sample and (b) single crystal crushed into a fine powder. The open circle shows the observed pattern, the dashed line shows the calculated pattern, the bottom line shows the difference pattern, and the markers represent the Bragg peak positions.

inhomogeneity as the origin of such magnetic anomalies. A recent work by Samal et al.[29,30] on polycrystalline samples reported that the occurrence of PS is greatly influenced by the preparation method and the most probable ground state of $La_{0.85}Sr_{0.15}CoO_3$ is SG. A brief preliminary study by Manna et al.[31] on single crystals also indicated the canonical SG behavior in $La_{0.85}Sr_{0.15}CoO_3$. Keeping abreast of all this information, we have investigated thoroughly the magnetic properties of the $La_{0.85}Sr_{0.15}CoO_3$ single crystal in order to have a deep understanding about the magnetic state associated with this system. In this article, we present experimental evidence to show that the magnetic ground state for $La_{0.85}Sr_{0.15}CoO_3$ is indeed SG in nature.

II. EXPERIMENTAL SECTION

A. Sample Preparation and Structural Characterization. The polycrystalline $La_{0.85}Sr_{0.15}CoO_3$ sample is synthesized by a standard solid-state reaction method using La_2O_3, CoC_2O_4, and $SrCO_3$ precursors. La_2O_3 is first preheated at 900 °C for 14 h in air, after which all the constituents are mixed in the stoichiometric ratio and heated in a Pt crucible at 900 °C for 24 h in air, followed by controlled cooling at the rate of 100 °C/h to room temperature. Subsequently, the material is heated again in two steps: first, at 1100 °C, and then at 1300 °C for 24 h each in air. During the heat treatment, the mixture is repeatedly ground at different stages for homogenization and to form a single phase. Structural characterization is performed by powder X-ray diffraction (XRD) at various stages of the preparation using a Bruker D8 advance X-ray diffractometer. Rietveld refinement using the general structure analysis system code (GSAS)[32] of the XRD pattern of the polycrystalline sample is shown in Figure 1a. It is found that the sample crystallizes in a rhombohedral $R\bar{3}c$ structure at room temperature. The lattice parameters "a" and "c" in the hexagonal setting are estimated as 5.447 and 13.153 Å, respectively, and are consistent with reported values.[33] The R_{wp}, R_p, and χ^2 factors obtained from the refinement are 0.022, 0.017, and 2.6, respectively. For the single-crystal growth, feed rods are prepared by pressing the polycrystalline material (diameter, ~6.5 mm; length, ~8.5 cm) up to 70 MPa using a hydrostatic press and subsequent sintering at 1400 °C for 24 h in air. The single crystal is grown in a float zone four-mirror optical image furnace (FZ-T-10000-H-VI-VP, Crystal Systems Inc., Japan) under 5 bar oxygen pressure and at a typical growth velocity of 3 mm/h. The feed rod and seed rotation rates were maintained at 35 and 30 rpm, respectively. The typical size of a grown crystal was ~6 mm (diameter) and ~57 mm (length). The powder X-ray diffraction with Rietveld refinement (using GSAS) of the grown crystal is shown in Figure 1b, which confirms that, within the sensitivity of XRD, the material is single phase. The lattice parameters a and c are estimated as 5.448 and 13.155 Å, respectively. The R_{wp}, R_p, and χ^2 factors are 0.0167, 0.0102, and 4.12, respectively. The Sr content that was determined by inductively coupled plasma-atomic emission spectroscopy (ICP-AES) agrees well with the chemical formula composition. The oxygen content probed by iodometric titration is found to be close to the stoichiometric composition. Single crystallinity is confirmed by Laue photography with the boule axis very close to the [111] direction. However, the crystal is found to be twinned as in the case of other distorted perovskites.

B. Measurement Details. The magnetization measurements are performed using a quantum design superconducting quantum interference device (SQUID) magnetometer in the temperature range of 10−300 K and a magnetic field up to 5 T. ac susceptibility measurements are performed by a commercial CryoBIND system down to 4.2 K and in the frequency range of 15 Hz to 1 kHz. Electrical and magnetotransport properties are measured using a standard four-probe Van der Pauw configuration in the magnetic field up to 11 T with silver−indium contacts. The magnetotransport studies are carried out using a configuration in which the current direction is perpendicular to the applied field. In all measurements, the field was applied along the boule axis, close to the [111] direction.

III. RESULTS AND DISCUSSION

A. dc Magnetization and Magnetotransport Study. The temperature-dependent field-cooled (FC) and zero-field-cooled (ZFC) magnetization (M_{FC} and M_{ZFC}) at 100 and 1000 Oe are shown in Figure 2a,b, respectively. Both FC curves display a kink below the corresponding freezing temperature (T_f), which is a characteristic feature of SG systems.[12] With the application of a higher dc field (1000 Oe), T_f shifts to lower value (from ~65 to ~58 K), which occurs due to the subtle balance between thermal and magnetic energy. The ZFC curve exhibits a sharp peak at T_f mostly governed by the SG dynamic transition.[12] In principle, a peak in the ZFC curve signifies either SG or antiferromagnetic behavior. However, in the SG system, the peak shifts to lower temperature as the dc field is increased. It is interesting to note from Figure 2 that the bifurcation between ZFC and FC curves occurs very close to T_f, as usually noticed in model SG systems.[12] Our finding is unlike to what has been observed by other groups[22,23] where the bifurcation occurs at the irreversibility temperature, (T_{irr}), where $T_{irr} \gg T_f$. Hence, the magnetization data support the existence of better compositional homogeneity in the present sample. Figure 3a,b illustrates $M-H$ curves at 10 and 100 K, respectively, for the $La_{0.85}Sr_{0.15}CoO_3$ single crystal. At 10 K, the coercive field (H_c) is ~0.616 T. However, at 100 K,

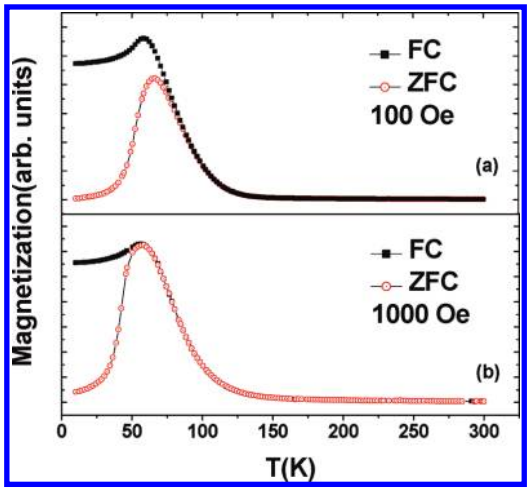

Figure 2. Temperature dependence of FC and ZFC dc magnetizations for the $La_{0.85}Sr_{0.15}CoO_3$ single crystal at (a) 100 and (b) 1000 Oe. FC curves are shown as solid symbols and ZFC curves as open symbols.

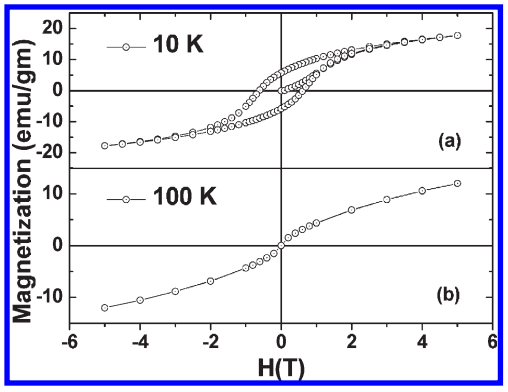

Figure 3. $M-H$ hysteresis curves for the $La_{0.85}Sr_{0.15}CoO_3$ single crystal at (a) 10 and (b) 100 K.

the system does not show any hysteresis because it is well above the SG ordering temperature. It is also interesting to note that the $M-H$ plot at 10 K does not seem to saturate at the 5 T field. The lack of saturation-like behavior even at a relatively high field once again indicates a typical SG behavior.[12]

Figure 4 shows the magnetoresistance (MR) variation of the $La_{0.85}Sr_{0.15}CoO_3$ single crystal, calculated as $(\rho(H) - \rho(H=0))/\rho(H=0)$, at different temperatures from 10 to 150 K. The inset shows the semiconducting-like (i.e., $(d\rho/dT) < 0$) behavior from 290 to 4.2 K. We have tried to fit the zero field resistivity data with the Mott variable range hopping (MVRH) conduction mechanism, that is, $\rho(T) = A \exp[(T_0/T)^{1/4}]$, where A and T_0 are constants. This was done with a view to understand the mode of electrical transport involved in this material. It is found that the data fit reasonably well to MVRH in a narrow window of temperature, that is, $\Delta T \sim 80$ K in the range from 70 to 150 K. However, when we consider the data spread over the entire temperature range in the paramagnetic region, it does not fit to any of the conventional hopping conduction mechanisms. It is also observed that the sample exhibits a huge negative MR of ~70% at about 10 K, which monotonically decreases with the increase of temperature. This emphasizes two important factors: (a) the value of MR does not saturate even at the applied field

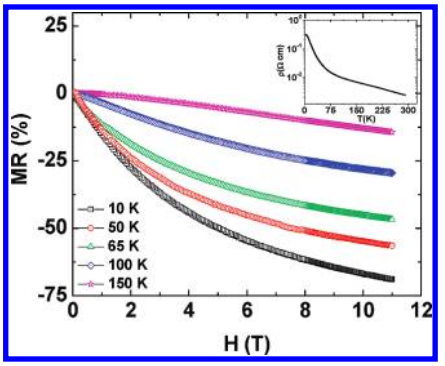

Figure 4. Magnetic field dependence of MR at different temperatures for the $La_{0.85}Sr_{0.15}CoO_3$ single crystal. The inset displays the temperature dependence of resistivity in $H = 0$ T.

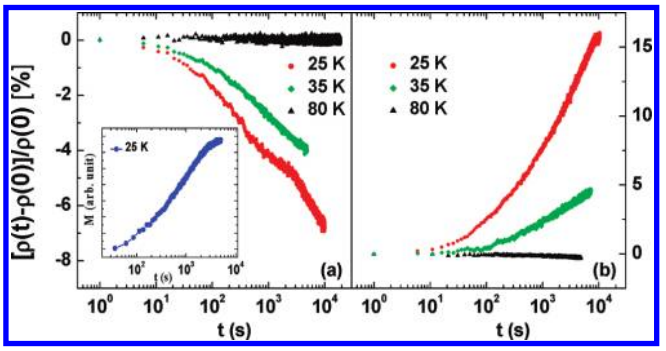

Figure 5. Time-dependent resistance variation at 25, 35, and 80 K after (a) ZFC from 100 K to the measuring temperature, then applying an 11 T magnetic field, and (b) FC with 11 T from 100 K to the same temperature and then removing the 11 T field. In case (a), the field reached 11 T in 670 s, and in case (b), it took 282 s to remove it. The inset shows the time evolution of magnetization at 25 K with an applied field of 5 T.

strength of 11 T and (b) MR increases sharply at low temperature with the increase in applied magnetic field. There is a strong hint that the MR scales with the sample's magnetization; that is, resistivity decreases sharply as M increases with the application of the magnetic field.

To understand the signature of glassy transport involved in this material, we have performed the resistivity relaxation study. Figure 5a demonstrates the response of resistance to the application of a magnetic field below and above T_f. In this measurement mode, the sample is cooled from 100 K to the measuring temperature (i.e., 25, 35, and 80 K) and then an 11 T field is applied and the response is noted with the progress of time. A large negative change in resistance, $[(\rho(t) - \rho(t=0))/\rho(t=0)] \sim (6-7\%)$, is observed with the evolution of time over a period of 10^4 s for $T < T_f$, and this behavior disappears for $T > T_f$. The time-dependent effect below T_f is believed to be due to the slow polarization of the glassy phase. When the field is held on for a sufficiently long time during the measurement, the randomly oriented spins tend to align slowly in the direction of the applied field with the progress of time. This process reduces the spin-dependent scattering probability because the system gradually improves its magnetic order. To check how the magnetization changes with the progress of time after the application of the magnetic field, we have carried out the magnetic

dx.doi.org/10.1021/jp201206a |J. Phys. Chem. C 2011, 115, 13985–13990

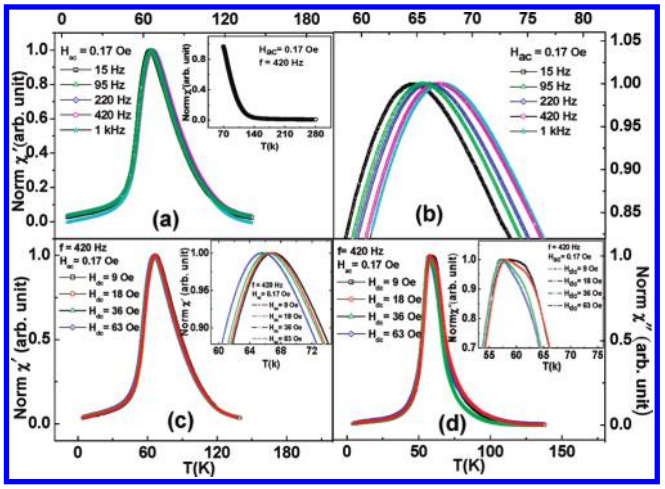

Figure 6. Temperature dependence of the in-phase (a) components of ZFC ac susceptibility for the $La_{0.85}Sr_{0.15}CoO_3$ single crystal at 15, 42, 95, 220, 420, and 1000 Hz. The inset shows the temperature dependence of the in-phase component of ac susceptibility at 420 Hz in the high-temperature range (from 70 to 280 K). (b) Zoom-in view of the temperature dependence of the in-phase components of ZFC ac susceptibility at various frequencies. Temperature dependence of the dc biased in-phase (c) and out-of-phase (d) components of ZFC ac susceptibility for the $La_{0.85}Sr_{0.15}CoO_3$ single crystal at 9, 18, 36, and 63 Oe dc fields. The insets in (c) and (d) show the zoom-in views of the peak shifts with respect to the dc biasing field.

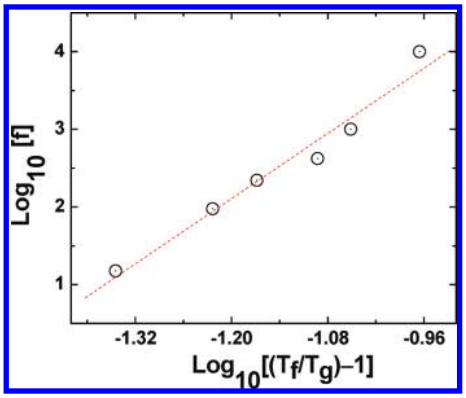

Figure 7. $\log_{10} f$ vs $\log_{10}[(T_f/T_g) - 1]$ for the $La_{0.85}Sr_{0.15}CoO_3$ single crystal. The dashed line represents the best fit to the data.

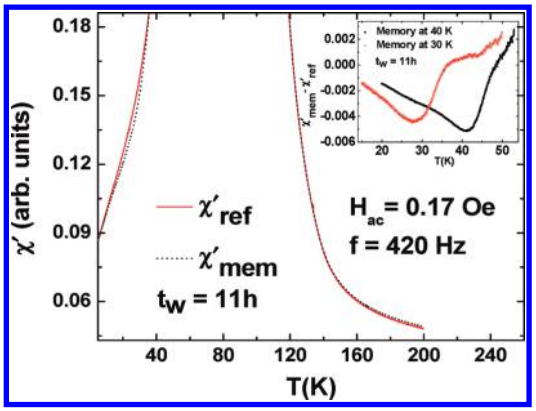

Figure 8. Magnified view of the temperature dependence of the in-phase ac susceptibility χ'_{ref} (reference curve) and on imprinting memory, χ'_{mem} (memory experiment). The inset shows a difference $(\chi'_{mem} - \chi'_{ref})$ plot of the in-phase ac susceptibility component at T_{halt} = 30 and 40 K with a halting time of $t_w \sim 11$ h.

relaxation study at 25 K with an applied magnetic field of 5 T. The experimental protocol for magnetic relaxation is the same as described above for resistivity relaxation. The inset in Figure 5a shows the evolution of magnetization with time. It is conspicuous that the magnetization tends to increase with the progress of time and thus corroborates the results concerning the time-dependent change in resistance as described above. Figure 5b represents the response to the removal of the magnetic field below and above the T_f. In this mode of measurement, the sample is field-cooled with an 11 T field from 100 K to the desired temperature. The field is then switched off, and the response is noted with the progress of time. It is evident that, after removal of the field, the system exhibits a positive change in resistance, $[(\rho(t) - \rho(t=0))/\rho(t=0)] \sim (15-16\%)$, with the evolution of time below T_f and the effect disappears above T_f, that is, at 80 K.

B. ac Susceptibility Study. Figure 6 illustrates normalized $\chi'(T)$ and $\chi''(T)$, that is, real and imaginary components of ac susceptibility (χ_{ac}), measured under different experimental conditions. Figure 6a represents the normalized $\chi'(T)$ up to 140 K at frequencies of f = 15, 42, 95, 220, 420, and 1000 Hz in an ac field, H_{ac}= 0.17 Oe. Figure 6b shows the enlarged view of Figure 6a around the peak positions. It is explicit that the sample exhibits a frequency-dependent peak shift. The peak position shifts to higher temperature with the increase in the frequency, a phenomenon commonly observed in SG systems.[22,29,30,34] The maximum shift in temperature $\Delta T_{max} = (T_f^{1\ kHz} - T_f^{15\ Hz})$ is ~4 K. A quantitative measurement of the frequency shift for $\chi'(T)$ can be obtained from $s = \Delta T_f/[T_f \Delta \log_{10} f] = 0.0225$, where $\Delta T_f = (T_{f1} - T_{f2})$ and $\Delta \log_{10} f = [\log_{10} f_1 - \log_{10} f_2]$ with f_1 = 1 kHz and f_2 = 15 Hz. The estimated value of "s" lies well within the reported range [0.0045−0.08].[35] The plot of $\chi'(T)$ from 70 to 280 K (inset of Figure 6a) shows no additional peak. Consequently, we rule out the possibility of any high-temperature magnetic phases. Besides, the frequency dependence of T_f can be described by the conventional "critical slowing down" model,[22,35−37] such as

$$\tau_f = \tau_0 (T_f/T_g - 1)^{-z\nu}$$

where T_g is the freezing temperature at $f \rightarrow 0$, $z\nu$ is a dynamicals exponent, τ_0 is the microscopic flipping time of fluctuating spins, and T_f is the freezing temperature at a particular given frequency f. The above equation is validated in Figure 7 where $\log_{10} f$ is plotted as a function of $\log_{10}[(T_f/T_g) - 1]$. The best fit is found to occur at $T_g \sim 61.9 \pm 0.6$ K with $\tau_0 = (4.9 \pm 0.6) \times 10^{-13}$ s and $z\nu = 8.6 \pm 0.4$. It is encouraging to note that the values obtained for the fitting parameters $z\nu$ and τ_0 are comparable to those reported for typical canonical SG systems.[22,35−37] Figure 6c,d represents $\chi'(T)$ and $\chi''(T)$ measured by applying different dc fields superposed on an ac field of H_{ac} = 0.17 Oe, at 420 Hz. We observe that T_f shifts to lower temperature with increasing superposed dc field. The shift is clearly seen in insets of Figure 6c,d. A possible explanation of this behavior is that the applied superposed dc field hinders the random reorganization process of the spin structure, thus shifting T_f to lower values.

To further corroborate the existence of SG behavior, we have investigated the time-dependent magnetic study. Though the

spins continuously reorganize themselves, the system does not reach the equilibrium state within the experimental time scale due to the slow dynamics. Consequently, this leads to nonequilibrium phenomena, such as memory and aging effects.[38] The memory effect is demonstrated by measuring χ'_{ac} in two different ways: one by reference measurement (χ'_{ref}) and another through memory experiment (χ'_{mem}). In the reference measurement, the sample is zero-field-cooled from a temperature well above T_f, that is, 300−4.2 K, and χ'_{ref} is measured by applying an ac magnetic field of 0.17 Oe with a frequency of 420 Hz during the heating run (up to 280 K at a rate of 2 K/min). In the memory experiment, the sample is zero-field-cooled from 280 to 4.2 K with an intermediate stop at a temperature T_{halt} below T_f for a time of $t_w = 11$ h. The χ'_{mem} is then measured while continuously heating the sample to 280 K at the same rate of 2 K/min with the same ac field and frequency. Figure 8 shows the enlarged view of the χ'_{ac} of both memory and reference measurements. To illustrate the memory effect more clearly, a comparative difference plot ($\chi'_{mem} - \chi'_{ref}$) is shown in the inset of Figure 8 for $T_{halt} \sim 30$ and 40 K. It is very clear that a dip occurs at around the waiting temperature, reflecting the memory effect in this compound. This behavior is very similar to that observed in other SG systems.[38] In summary, the frequency-dependent peak shift, a pronounced memory effect, and the relaxation time τ_0 [$\sim 10^{-13}$ s] constitute strong evidence of the existence of SG dynamics in this compound.

IV. CONCLUSION

We have performed structural, dc magnetization, ac susceptibility, and magnetotransport measurements on $La_{0.85}Sr_{0.15}CoO_3$ single crystals. The XRD pattern of the crushed single crystal confirms the phase purity. Many characteristics of canonical SG systems are discernible in the magnetic study of $La_{0.85}Sr_{0.15}CoO_3$, such as a kink in the field-cooling curve below T_f, a frequency-dependent peak shift, and the time-dependent memory effect. The relaxation time for the system is observed in the subpicosecond range ($\sim 10^{-13}$ s), which is very similar to that in noble spin-glass systems. Most remarkably, our experimental results do not find any signature of the presence of T_{irr} arising out of ferromagnetic clusters. In addition, we also observe the time evolution of resistance in response to the magnetic field below T_f, as is expected for SG systems. On the basis of these results, we strongly believe that the most probable magnetic ground state for $La_{0.85}Sr_{0.15}CoO_3$ is SG in nature.

AUTHOR INFORMATION

Corresponding Author

*E-mail: anil@physics.iisc.ernet.in.

ACKNOWLEDGMENT

We gratefully acknowledge the use of the National Facility for Low Temperature and High Magnetic Fields (LTHMF), IISc, for magnetotransport measurements. We also acknowledge the financial support of the Department of Science and Technology (DST), Govt. of India, for providing funds to carry out this research work. K.M. acknowledges the Council of Scientific and Industrial Research (CSIR), Govt. of India, for providing the scholarship.

REFERENCES

(1) Roder, H.; Zang, J.; Bishop, A. R. *Phys. Rev. Lett.* **1996**, *76*, 1356.
(2) Zhao, G.; Conder, K.; Keller, H.; Muller, K. A. *Nature* **1996**, *381*, 676.
(3) Tokura, Y.; Tomioka, Y. *J. Magn. Magn. Mater.* **1999**, *200*, 1.
(4) Salamon, M. B.; Jaime, M. *Rev. Mod. Phys.* **2001**, *73*, 583.
(5) Lee, P. A.; Nagaosa, N.; Xiao-Gang, W. *Rev. Mod. Phys.* **2006**, *78*, 17.
(6) Senarisrodriguez, M. A.; Goodenough, J. B. *J. Solid State Chem.* **1995**, *118*, 323.
(7) Baier, J.; Jodlauk, S.; Kriener, M.; Reichl, A.; Zobel, C.; Kierspel, H.; Freirnuth, A.; Lorenz, T. *Phys. Rev. B* **2005**, *71*, 014443.
(8) Raccah, P. M.; Goodenough, J. B. *Phys. Rev.* **1967**, *155*, 932.
(9) Asai, K.; Yokokura, O.; Nishimori, N.; Chou, H.; Tranquada, J. M.; Shiranem, G.; Higuchi, S.; Okajima, Y.; Kohn, K. *Phys. Rev. B* **1994**, *50*, 3025.
(10) Yamaguchi, S.; Okimoto, Y.; Tokura, Y. *Phys. Rev. B* **1997**, *55*, 8666(R).
(11) Haverkort, M. W.; Hu, Z.; Cezar, J. C.; Burnus, T.; Hartmann, H.; Reuther, M.; Zobel, C.; Lorenz, T.; Tanaka, A.; Brookes, N. B.; Hsieh, H. H.; Lin, H.-J.; Chen, C. T.; Tjeng, L. H. *Phys. Rev. Lett.* **2006**, *97*, 176405.
(12) Mydeen, K.; Mandal, P.; Prabhakaran, D.; Jin, C. Q. *Phys. Rev. B* **2009**, *80*, 014421.
(13) Kriener, M.; Zobel, C.; Reichl, A.; Baier, J.; Cwik, M.; Berggold, K.; Kierspel, H.; Zabara, O.; Freimuth, A.; Lorenz, T. *Phys. Rev. B* **2004**, *69*, 094417.
(14) Caciuffo, R.; Rinaldi, D.; Barucca, G. l.; Mira, J.; Rivas, J.; Senarisrodriguez, M. A.; Radaelli, P. G.; Fiorani, D.; Goodenough, J. B. *Phys. Rev. B* **1999**, *59*, 1068.
(15) Itoh, M.; Natori, I.; Kubota, S.; Motoya, K. *J. Phys. Soc. Jpn.* **1994**, *63*, 1486.
(16) Senarisrodriguez, M. A.; Goodenough, J. B. *J. Solid State Chem.* **1995**, *116*, 224.
(17) Sathe, V. G.; Pimpale, A. V.; Siruguri, V.; Paranjpe, S. K. *J. Phys.: Condens. Matter* **1996**, *8*, 3889.
(18) Kuhns, P. L.; Hoch, M. J. R.; Moulton, W. G.; Reys, A. P.; Wu, J.; Leighton, C. *Phys. Rev. Lett.* **2003**, *91*, 127202.
(19) Wu, J.; Lynn, J. W.; Glinka, C. J.; Burley, J.; Zheng, H.; Mitchell, J. F.; Leighton, C. *Phys. Rev. Lett.* **2005**, *94*, 037201.
(20) Tang, Y. K.; Sun, Y.; Cheng, Z. H. *Phys. Rev. B* **2006**, *73*, 012409.
(21) Rivadulla, F.; Lopez-Quintela, M. A.; Rivas, J. *Phys. Rev. Lett.* **2004**, *93*, 167206.
(22) Wu, J.; Leighton, C. *Phys. Rev. B* **2003**, *67*, 174408.
(23) Phuc, N. X.; Khiem, N. V.; Hoai, Nam, D. N. *J. Magn. Magn. Mater.* **2002**, *242−245*, 754.
(24) Burgy, J.; Mayr, M.; Martin-Mayor, V.; Moreo, A.; Dagotta, E. *Phys. Rev. Lett.* **2001**, *87*, 277202.
(25) Aarbogh, H. M.; Wu, J.; Wang, L.; Zheng, H.; Mitchell, J. F.; Leighton, C. *Phys. Rev. B* **2006**, *74*, 134408.
(26) Wu, J.; Zheng, H.; Mitchell, J. F.; Leighton, C. *Phys. Rev. B* **2006**, *73*, 020404(R).
(27) Mira, J.; Rivas, J.; Baio, G.; Barucca, G.; Rinaldi, D.; Fiorani, D.; Senarisrodriguez, M. A. *J. Appl. Phys.* **2001**, *89*, 5606.
(28) Anil Kumar, P. S.; Joy, P. A.; Date, S. K. *J. Appl. Phys.* **1998**, *83*, 7375.
(29) Samal, D.; Shivakumara, C.; Anil Kumar, P. S. *J. Appl. Phys.* **2009**, *106*, 123920.
(30) Samal, D.; Balamurugan, K.; Shivakumara, C.; Anil Kumar, P. S. *J. Appl. Phys.* **2009**, *105*, 07E320.
(31) Manna, K.; Samal, D.; Elizabeth, S.; Bhat, H. L.; Anil Kumar, P. S. *J. Supercond. Novel Magn.* **2011**, *24*, 833.
(32) (a) Larson, A. C.; von Dreele, R. B. *General Structure Analysis System*; Los Alamos National Laboratory: Los Alamos, NM, 2000; pp 86−748. (b) Toby, B. H. *J. Appl. Crystallogr.* **2001**, *34*, 210.
(33) Sikolenko, V. V.; Pomjakushina, E. V.; Istomin, S. Ya. *J. Magn. Magn. Mater.* **2003**, *258−259*, 300.

(34) Cardoso, C. A.; Araujo-Moreira, F. M.; Awana, V. P. S.; Takayama-Muromachi, E.; de Lima, O. F.; Yamauchi, H.; Karppinen, M. *Phys. Rev. B* **2003**, *67*, 020407(R).
(35) Mydosh, J. A. *Spin Glasses: An Experimental Introduction*; Taylor & Francis: London, 1993.
(36) Gunnarsson, K.; Svedlindh, P.; Nordblad, P.; Lundgren, L. *Phys. Rev. Lett.* **1988**, *61*, 754.
(37) Wang, F.; Kim, J.; Kim, Y. J. *Phys. Rev. B* **2009**, *80*, 024419.
(38) Kundu, A. K.; Nordblad, P.; Rao, C. N. R. *J. Phys.: Condens. Matter* **2006**, *18*, 4809. *Phys. Rev. B* **2006**, *72*, 144423.